Amino Acids (2010) 39:243–255
DOI 10.1007/s00726-009-0434-5

ORIGINAL ARTICLE

Generation of in silico predicted coxsackievirus B3-derived MHC class I epitopes by proteasomes

Antje Voigt · Sandra Jäkel · Kathrin Textoris-Taube · Christin Keller · Ilse Drung · Gudrun Szalay · Karin Klingel · Peter Henklein · Karl Stangl · Peter M. Kloetzel · Ulrike Kuckelkorn

Received: 10 August 2009 / Accepted: 19 November 2009 / Published online: 9 December 2009

Abstract Proteasomes are known to be the main suppliers of MHC class I (MHC-I) ligands. In an attempt to identify coxsackievirus B3 (CVB3)-MHC-I epitopes, a combined approach of in silico MHC-I/transporters associated with antigen processing (TAP)-binding and proteasomal cleavage prediction was applied. Accordingly, 13 potential epitopes originating from the structural and non-structural protein region of CVB3 were selected for further in vitro processing analysis by proteasomes. Mass spectrometry demonstrated the generation of seven of the 13 predicted MHC-I ligands or respective ligand precursors by proteasomes. Detailed processing analysis of three adjacent MHC-I ligands with partially overlapping sequences, i.e. VP2(273–281), VP2(284–292) and VP2(285–293), revealed the preferential generation predominantly of the VP2(285–293) epitope by immunoproteasomes due to altered cleavage site preferences. The VP2(285–293) peptide was identified to be a high affinity binder, rendering VP2(285–293) a likely candidate for CD8 T cell immunity in CVB3 infection. In conclusion, the concerted usage of different in silico prediction methods and in vitro epitope processing/presentation studies was supportive in the identification of CVB3 MHC-I epitopes.

Keywords Proteasomes · Epitope prediction · Antigen processing · Coxsackievirus

Electronic supplementary material The online version of this article (doi:10.1007/s00726-009-0434-5) contains supplementary material, which is available to authorized users.

A. Voigt · K. Stangl
Clinic for Cardiology and Angiology,
Charité-Universitätsmedizin Berlin,
Campus Mitte, 10117 Berlin, Germany

S. Jäkel · K. Textoris-Taube · C. Keller · I. Drung · P. Henklein · P. M. Kloetzel (✉) · U. Kuckelkorn
Institut für Biochemie CC2, Charité-Universitätsmedizin Berlin,
Monbijoustrasse 2, 10117 Berlin, Germany
e-mail: p-m.kloetzel@charite.de

G. Szalay · K. Klingel
Department of Molecular Pathology, University of Tübingen,
72076 Tübingen, Germany
e-mail: gudrun.szalay@gmx.de

Present Address:
G. Szalay
Paul-Ehrlich institut, 63225 Langen, Germany

Introduction

Coxsackievirus B3 (CVB3)-infection is a frequent cause of acute myocarditis. In about 20% of patients viral myocarditis leads to its sequela dilated cardiomyopathy (DCM), which is linked to chronic inflammation and persistence of cardiotropic viruses (Liu and Mason 2001; Mason 2003). A murine model of CVB3-myocarditis has been established to study the course of myocarditis in detail (Klingel et al. 1992; Szalay et al. 2006). CD8 T cells are crucial in the control of acute inflammation in CVB3-infection (Henke et al. 1995; Klingel et al. 2003). CD8 T cells discriminate between normal and virus infected cells on the basis of the repertoire of peptides presented on the cell surface by MHC class I molecules (MHC-I) (Kloetzel 2001). The number of potentially generated antigenic peptides within the viral genome is extremely large, however, de facto only a small amount of antigenic peptides is eventually presented on the cell surface (Princiotta et al. 2003). The presentation of peptides on MHC class I molecules prerequisites different aspects: the initial generation of antigenic peptides from viral proteins; the transport of

generated peptides into the endoplasmic reticulum (ER) via transporters associated with antigen processing (TAP); the affinity of these peptides to MHC-I and the stability of MHC-I-peptide complexes, respectively (Chen et al. 2001; Fruci et al. 2003; Su and Miller 2001).

The vast majority of MHC-I ligands are processed by proteasomes (Kloetzel 2001). The length of the generated peptides varies between 3 and 30 residues (Kisselev et al. 1999). Due to cleavage site preferences proteasomes predominantly generate the correct C-terminal end of antigenic peptides. Peptides with correct size and proper amino acid sequence motifs are transported into the ER and bind to MHC-I in order to be transferred to the cell surface (Kloetzel 2001). Peptide transporters (TAP) also exert high binding affinities to N-terminally elongated MHC-I ligands (Fruci et al. 2003). These peptides are eventually trimmed at their N-terminus by peptidases within the ER resulting in perfect fit of antigenic peptides into the MHC-I binding grove (Beninga et al. 1998; Cascio et al. 2001).

The 20S proteasome is the catalytic core of the 26S proteasome, which is responsible for the degradation of polyubiquitylated proteins (Rechsteiner et al. 1993; Voges et al. 1999). The catalytic activity within the 20S core proteasome is restricted to the three inner beta subunits, i.e. β1, β2 and β5 with preferential cleavage after acidic, basic and hydrophobic amino acids, respectively (Groll et al. 1997). Upon interferon-stimulation three alternative catalytic proteasome subunits (β1i, β2i and β5i) that exert altered cleavage characteristics are incorporated into the 20S proteasome core, thus forming the immunoproteasome (i20S) (Aki et al. 1994; Griffin et al. 1998). Detailed studies on the functional importance of i20S revealed that in particular the generation and presentation of viral epitopes is strongly enhanced in the presence of i20S and that their function is tightly connected with the early phases of an antiviral immune response (Schwarz et al. 2000; Sijts et al. 2000; Strehl et al. 2006).

Within the last years different computational methods were developed that allow the prediction of T cell epitopes. Main criteria for prediction are the correct size of the peptides for MHC-I binding between 8 and 11 residues dependent on the MHC-I allele and the fulfillment of MHC-I allele binding properties by distinct amino acid residues. SYFPEITHI database comprises more than 4,500 peptide sequences known to bind to MHC class I and class II molecules (Rammensee et al. 1999). Further improvement of prediction results was obtained by additional prediction analysis for the peptide transport via TAP into the ER (Peters et al. 2003). Immune epitope database analysis resource (IEDB-AR) implements these different tools and methods for the prediction and analysis of immune epitopes (Zhang et al. 2008). The prediction of proteasomal cleavage remains to be challenging. NetChop and PAProC provide C-terminal cleavage sites of ligands by the proteasome, which often corresponds to the C-terminus of MHC-I peptides (Kuttler et al. 2000; Toes et al. 2001). However, the generation of the N-terminus of MHC-I ligands is a complex process making reliable prediction difficult.

In the present study, we attempted to identify CVB3 $CD8^+$ T cell epitopes with a particular focus on proteasomal generation of these epitopes. On the basis of prediction methods, polypeptides harboring 13 predicted MHC-I ligands from the structural and non-structural protein region of CVB3 were subjected to in vitro proteasomal processing studies and analyzed by mass spectrometry. These analyses revealed the proteasomal generation for 7 of the 13 predicted MHC-I ligands or respective ligand precursors. Exemplary analysis of peptide processing of adjacent MHC-I ligands with partially overlapping sequences revealed that the VP2(285–293) epitope, which exerted a relatively high MHC-I binding affinity, was preferentially generated by immunoproteasomes due to altered cleavage site preferences.

Results

Prediction of CVB3 MHC-I ligands

In an attempt to identify potential murine CD8 T cell epitopes derived from CVB3, different computational approaches were applied: SYFPEITHI database assigns an overall likelihood of a peptide of being a natural MHC ligand (Rammensee et al. 1999), IEDB-AR provides access to well-documented epitope-related tools through a common style of web interface comprising proteasomal cleavage as well as TAP and MHC-I binding probability (Peters et al. 2003; Zhang et al. 2008). H-2^b restricted peptides revealing high scores in SYFPEITHI and IEDB-AR, which were allocated to structural capsid proteins, i.e. VP2, VP3 and VP4, and to non-structural proteins, i.e. P2C, P3C and P3D of CVB3 polyprotein were selected for in vitro processing studies by proteasomes. In detail, 12 peptides were randomly selected from different parts of the CVB3 polyprotein on the basis of these inclusion criteria: (a) peptides with a SYFPEITHI score of $\geq$21 and $\leq$24 and a proteasome cleavage score as provided by IEDB-AR of $\geq$1.0 for s20S or i20S proteasomes of both H-$2K^b$ and H-$2D^b$ background and (b) peptides with a SYFPEITHI score of $\geq$25 with a proteasome cleavage score $\geq$1.0 [except VP2(285–293): proteasomal cleavage score 0.99] (Table 1). IEDB revealed low or intermediate MHC-I binding probability for most of the potential H-$2D^b$-restricted CVB3 epitopes, which was somewhat contradictory to the score assigned to different peptides by SYFPEITHI. Thus, we focused on SYFPEITHI database to determine the likelihood of a CVB3 peptide to be a natural MHC ligand.

Table 1 Prediction scores of potential CVB3 epitopes and generation of predicted MHC-I ligands by proteasomes

Position in CVB3 Nancy	Sequence	MHC class I haplotype	SYFPEITHI[A]	MHC affinity[B] IC50 (nM)	TAP[B] score	Proteasome cleavage prediction[B]		Proteasome in vitro generation	
						s20S score	i20S score	Epitope	Precursor peptide
VP4 (38–46)	SNSANRQDF	D^b	21	8,003.6	1.12	0.87	1.06	+	–
VP2 (153–161)	DALSNLGLF	D^b	27	778.5	0.93	0.84	1.21	–	–
VP2 (248–256)	VGVGNLTIF	D^b	26	1,997.3	1.03	0.93	1.33	–	–
VP2 (263–271)	LRTNNSATI	D^b	21	3,383.4	0.37	0.95	1.17	–	–
VP2 (284–292)	MFRHNNVTL	D^b	21	4,569.9	0.59	1.27	1.83	–	+
VP2 (285–293)	FRHNNVTLM	D^b	25	631.7	0.21	0.96	0.99	+	–
VP3(370–378)	GEVKNLMEI	D^b	27	3,063.1	0.06	0.93	1.17	+	+
P2C (1175–1183)	QLFSNVQYF	D^b	22	2,832.4	1.09	1.10	1.47	+	+
P3D (1901–1910)	ASSLNDSVAM	D^b	25	7,904.4	0.14	1.00	1.17	(–)	–
VP2 (128–135)	ATCRFYTL	K^b	23	52.5	0.49	1.12	1.50	–	–
P3C (1561–1568)	EYGEFTML	K^b	22	7,728.6	0.38	1.12	1.70	–	+
P3D (2170–2177)	TLPAFSTL	K^b	23	387.5	0.43	1.15	1.47	+	+
VP2 (273–281)[C]	MPYTNSVPM	D^b	22	565.5	0.12	0.83	0.72	–	–

[A] SYFPEITHI scores (Rammensee et al. 1999) and [B]IEDB-AR scores (all remaining scores, all Smm) (Zhang et al. 2008) are shown for the selected 12 MHC-I ligands (9 H-$2D^b$ and 3 H-$2K^b$ peptides) from the CVB3 polyprotein; selection criteria are described in the result section. [C]VP2(273–281) peptide, which is in close neighborhood to other predicted ligands like VP2(263–271), VP2(284–292) and VP2(285–293),was analyzed as well although proteasome cleavage probability was below the selected threshold. In the right columns epitope generation as determined by in vitro proteasomal processing studies is illustrated: + epitope and/or precursor detected in ESI/MS–MS; − epitope and/or precursor not detected in ESI/MS–MS; (–) not detected, but flanking fragments were identified

Particularly peptides originating from the VP2 protein at the N-terminus of the CVB3-polyprotein were found to be in close neighborhood to each other or even revealed a partial peptide sequence overlap, thus making the VP2 region a highly probable candidate for CVB3 epitope location. We also included the VP2(273–281) peptide (low proteasomal cleavage probability, but intermediate MHC-I binding predicted) due to the close neighborhood to other predicted ligands like VP2(263–271), VP2(284–292) and VP2(285–293). Also, the considerably high abundance of potential epitopes within a short part of the CVB3 polyprotein sequence raised the question, whether proteasomes are indeed able to generate all these peptides with a comparable efficiency or whether proteasomal cleavages rather result in the preferential generation of a selected number of these predicted MHC-I ligands. The 13 selected CVB3 MHC-I ligands and their respective prediction scores are depicted in Fig. 1 and Table 1.

Generation of predicted CVB3 MHC-I ligands by proteasomes

For processing analysis, 24–44mer polypeptides comprising the predicted MHC-I ligands and flanking peptide regions were synthesized. In vitro degradation of these peptides was performed with standard 20S proteasomes (s20S) (Suppl. Fig. (1)). ESI–MS/MS analysis of peptide digests revealed the generation of five out of the 13 selected MHC-I ligands, i.e. VP4(38–46), VP2(285–293), VP3(370–378), P2C(1175–1183), and P3D (2170–2177) as depicted in Fig. 2 and Table 1. Although epitope detection failed for VP2(284–292) and for P3C(1561–1568), we detected alternative, N-terminally elongated peptide (precursor peptide) generation by proteasomes for these MHC-I ligands.

We were not able to detect the remaining 6 selected MHC-I ligands in proteasomal processing studies by ESI–MS. Proteasomal generation of MHC-I ligands may also depend on flanking sequences or may fail, whenever N-termini of synthetic polypeptide substrates are too short for effective processing. To preclude these potential negative influences, we modified the sequence section for VP2(248–256), VP2(263–271) and VP2(273–281), which were investigated within the context of different polypeptide sequences (Fig. 2). Despite elongated N-terminal sequences, the detection of epitopes or precursor peptides for all three predicted MHC-I ligands failed in these experiments. Moreover, cleavage sites appeared to be abundant within the context of different flanking residues. In accordance to cleavage patterns observed for VP2(258–302), proteasomal degradation of VP2(267–290) revealed a cleavage behind V279 by proteasomes resulting in VP2(273–281) epitope destruction, thus correlating with the low proteasome cleavage prediction score by IEDB-AR for this additionally analyzed epitope (Table 1).

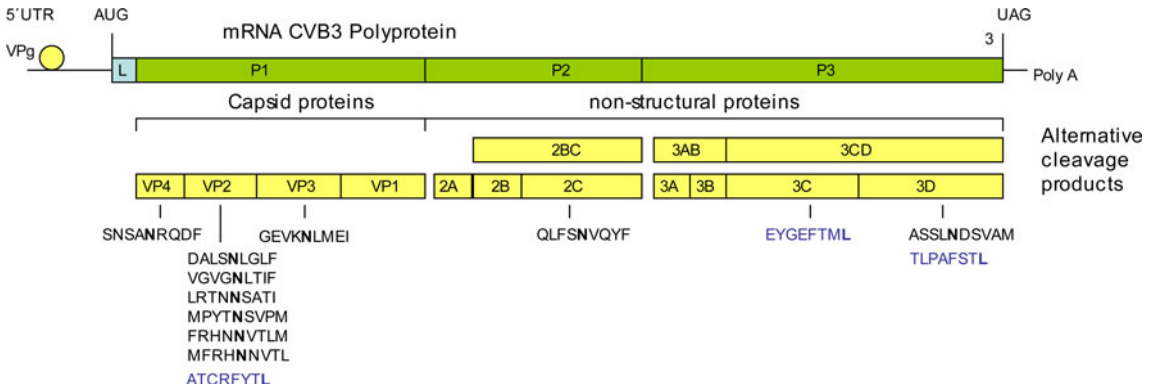

Fig. 1 Scheme of the CVB3-genome and translation products. The un-translated regions (*UTR*) at the 5′ and 3′ end, the P1 region for structural proteins, and the P2 and P3 regions for nonstructural proteins are shown. Translation products and their processing products yielding several intermediates and mature proteins are depicted below. The 13 selected MHC-I ligands are shown at the *bottom* with respect to their association to mature proteins (*black* H-2D^b; *blue* H-2K^b haplotype) (colour figure online)

	MHC ligand		Sequence (peptide) context
epitope detected	SNSANRQDF	$VP4_{32-55}$	YYKDAASNSANRQDFTQDPGKFTE
	FRHNNVTLM	$VP2_{272-302}$	VMPYTNSVPMDNMFRHNNVTLMVIPFVPLDY
	GEVKNLMEI	$VP3_{362-385}$	VTPEMRIPGEVKNLMEIAEVDSVV
	QLFSNVQYF	$P2C_{1161-1190}$	ATIEQSAPSQSDQEQLFSNVQYFAHYCRKY
	TLPAFSTL	$P3D_{2158-2185}$	RKIRSVPVGRCLTLPAFSTLRRKWLDSF
only precursor detected	MFRHNNVTL	$VP2_{272-302}$	VMPYTNSVPMDNMFRHNNVTLMVIPFVPLDY
	EYGEFTML	$P3C_{1549-1576}$	AMMKRNSSRVKTEYGEFTMLGIYDRWAV
no epitope/precursor detected	ATCRFYTL	$VP2_{116-141}$	*-ATAEDQPTQPDVATCRFYTLDSVQWQ
	DALSNLGLF	$VP2_{146-170}$	GWWWKLPDALSNLGLFGQNMQYHYL
	VGVGNLTIF	$VP2_{238-262}$ $VP2_{241-286}$	QRVYNAGMGVGVGNLTIFPHQWINL VYNAGMGVGVGNLTIFPHQWINLRTNNSATIVMPYTNSVPMDNMFR
	LRTNNSATI	$VP2_{258-302}$ $VP2_{241-286}$	HQWINLRTNNSATIVMPYTNSVPMDNMFRHNNVTLMVIPFVPLDY VYNAGMGVGVGNLTIFPHQWINLRTNNSATIVMPYTNSVPMDNMFR
	MPYTNSVPM	$VP2_{267-290}$ $VP2_{258-302}$ $VP2_{241-286}$	NSATIVMPYTNSVPMDNMFRHNNV HQWINLRTNNSATIVMPYTNSVPMDNMFRHNNVTLMVIPFVPLDY VYNAGMGVGVGNLTIFPHQWINLRTNNSATIVMPYTNSVPMDNMFR
	ASSLNDSVAM	$P3D_{1892-1917}$	AKGKSRLIEASSLNDSVAMRQTFGNL

Fig. 2 Processing of polypeptides by proteasomes. Synthetic polypeptides of different length harboring the predicted MHC-I ligands from the structural (VP) region and from the non-structural region of the CVB3 polyprotein (epitopes underlined) were conveyed to in vitro proteasomal digests with s20S and i20S proteasomes. Epitopes were identified by ESI–MS/MS. *First row* predicted MHC-I ligands (*underlined*) found as cleavage products in proteasome digests; *second row* predicted MHC-I ligands (*underlined*) not found as cleavage products in proteasome digests, but detection of respective precursor peptides by MS; *third row* predicted cleavage products not identified in proteasome digests. Generated peptides were identified in the s20S as well as in i20S proteasome digest. *Asterisk* indicates a PEG (polyethylene glycol) modification used to improve peptide solubility

Probably due to solubility restrictions of VP2(116–141), the degradation of this polypeptide substrate was not possible. To increase the solubility, this peptide was modified at the N-terminus with PEG (polyethylene glycol), thereby increasing its degradation rate. Four cleavages were observed within the predicted epitope sequence (data not shown). Thus, in contrast to considerably high cleavage prediction scores (Table 1), in vitro processing of

VP2(128–135) by proteasomes was not confirmed. Although identification of P3D(1901–1910) by ESI–MS/MS was inconclusive, we were able to identify both epitope-flanking sequences. Thus, one can assume in vitro proteasomal generation of P3D(1901–1910), although final proof is missing. In conclusion, we were able to detect the definite proteasomal generation for 5 of 13 predicted CVB3 MHC-I ligands tested here, whereby for two additional MHC-I ligands precursor peptide generation was observed.

Analysis of competing cleavage site usage by immunoproteasomes

The immunoproteasome was shown to crucially determine the antigen processing kinetics of epitopes (Deol et al. 2007). To study whether the quality of the peptides generated from the polypeptide substrates is dependent on i20S proteasomes, peptide fragments generated by the two proteasome types, i.e. s20S and immunoproteasomes (i20S) were compared. We did not observe any major qualitative differences in the peptide sequences of generated CVB3 peptides in the s20S and i20S proteasome processing studies suggesting the generation of identical peptides by both proteasome types (data not shown). The lack of changes in the quality of peptide generation was opposed to tremendous differences in peptide quantities generated by either s20S or i20S proteasomes. This quantitative effect of peptide generation may be particularly important for adjacent and partially overlapping epitope sequences, where the function of i20S proteasomes may potentially influence the immunogenicity of one particular epitope.

To study this effect in more detail, we focused on the impact of s20S and i20S proteasomes on MHC-I ligand generation of adjacent and partially overlapping epitope sequences, which were derived from the VP2(258–302) polypeptide (Fig. 2). This peptide substrate harbors four predicted MHC-I ligands, whereby two of these ligands have a peptide sequence overlap. In vitro processing of VP2(258–302) by s20S proteasome resulted exclusively in the generation of the VP2(285–293) MHC-I ligand. Taking into account the effect of different flanking sequences on cleavage site usage, we consequently studied peptide processing within the context of shorter flanking sequences using the synthetic peptide VP2(272–302), which harbors VP2(273–281), VP2(284–292) and VP2(285–293) (Fig. 3). Whereas the predicted epitope VP2(285–293) was detected in the peptide pool generated from VP2(258–302) and VP2(272–302), the overlapping MHC-I ligand VP2(284–292) was detected exclusively as a N-terminally elongated precursor peptide in the VP2(272–302) fragmentation study (Fig. 3).

Both overlapping sequences, the VP2(285–293) and VP2(284–292) peptide, were predicted to be likely CVB3 MHC-I epitopes; however, MHC-I affinity prediction suggested the VP2(285–293) epitope to be more affine than the VP2(284–292) epitope [VP2(285–293): SYFPEITHI score 25; IC_{50} 631.7] versus VP2(284–292): [SYFPEITHI score 21; IC_{50} 4,569.9]. In contrast, proteasome-processing scores suggested an improved generation of the VP2(284–292) epitope [i20S processing score 1.83 for VP2(284–292) versus 0,99 for VP2(285–293)] (Table 1). To investigate these two overlapping MHC-I ligands in detail, the degradation kinetic of the 31mer polypeptide VP2(272–302) harboring these two predicted epitopes was studied. Three main cleavage sites were identified, which are involved in epitope generation: M284/F285, L292/M293, and M293/V294. Both, the VP2(285–293) epitope and a 13mer VP2(284–292) precursor peptide were generated by s20S and i20S proteasomes (Figs. 3, 4). Remarkably, i20S revealed an accelerated turnover of 31mer polypeptide VP2(272–302) (Fig. 4a). As shown in Fig. 4b, c, i20S generated both the VP2(285–293) epitope, and the 13mer precursor peptide of VP2(284–292) i.e. VP2(280–292) with increased efficiency. In addition, the generation of the N- and C-terminal flanking residues of VP2(285–293) and of VP2(280–292) was likewise enhanced by i20S proteasomes.

The enhanced liberation of the epitope or precursor peptides may have been either due to the overall enhanced substrate turnover by i20S and/or due to altered cleavage site preferences of i20S, which may favor the liberation of individual peptides. To address this issue, we previously established a method comparing epitope generation versus the simultaneous generation of an alternative peptide within the context of the same degradation experiment (the so-called antitope), which precludes the generation of the correct epitope sequence and resulted in an non-functional peptide (Strehl et al. 2008). The antitope may lack the correct C-terminal residue of the epitope, but may share the N-terminal residue with the functional peptide or vice versa (Strehl et al. 2008). Figure 4d illustrates the ratios of VP2(285–293) epitope generation in s20S and i20S proteasome fragmentation studies compared to antitope peptide liberation. In fact, we observed a preferential generation of VP2(285–293) epitope by i20S proteasomes in comparison to respective antitope peptides. Standardisation of VP2(285–293) epitope to antitopes N283–V290, T291–V294 and F285–V290 revealed that i20S favoured the generation of the N- and the C-terminal proteasomal cleavage of theVP2(285–293) epitope (Fig. 4d). On the other hand, the ratio of VP2(285–293) epitope to antitope F285–L292 revealed no preference in the generation of either fragment by i20S. Whenever the generation of the 13mer precursor peptide of VP2(284–292) was analyzed in

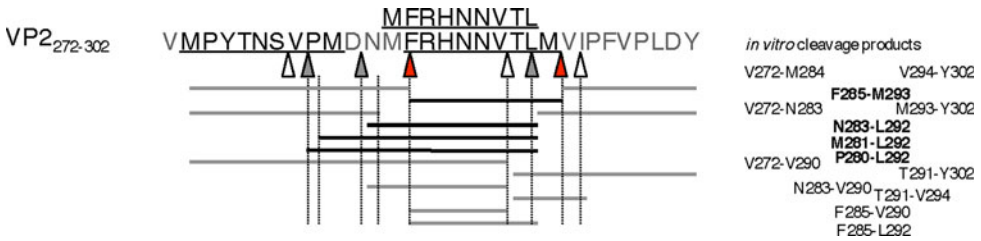

Fig. 3 Analysis of cleavage sites within the VP2 region. Based on the 44mer polypeptide CVB3 $VP2_{258–302}$, a shorter synthetic polypeptide harboring the potential MHC ligands VP2(273–281), VP2(284–292) and VP2(285–293) was processed by proteasomes and analyzed by ESI–MS/MS. The predicted MHC-I ligands are underlined. *Color arrows* pointing upward indicate major cleavage sites leading to the VP2(285–293) epitope generation (*red*) and to the VP2(284–292) precursor peptide generation (*gray*). *White arrows* indicate additional cleavage sites. The epitope-flanking fragments and these generated fragments, which share part of the epitope sequences ("antitopes"), are represented by *gray bars*. Cleavage sites generating VP2(273–281) were not detected (colour figure online)

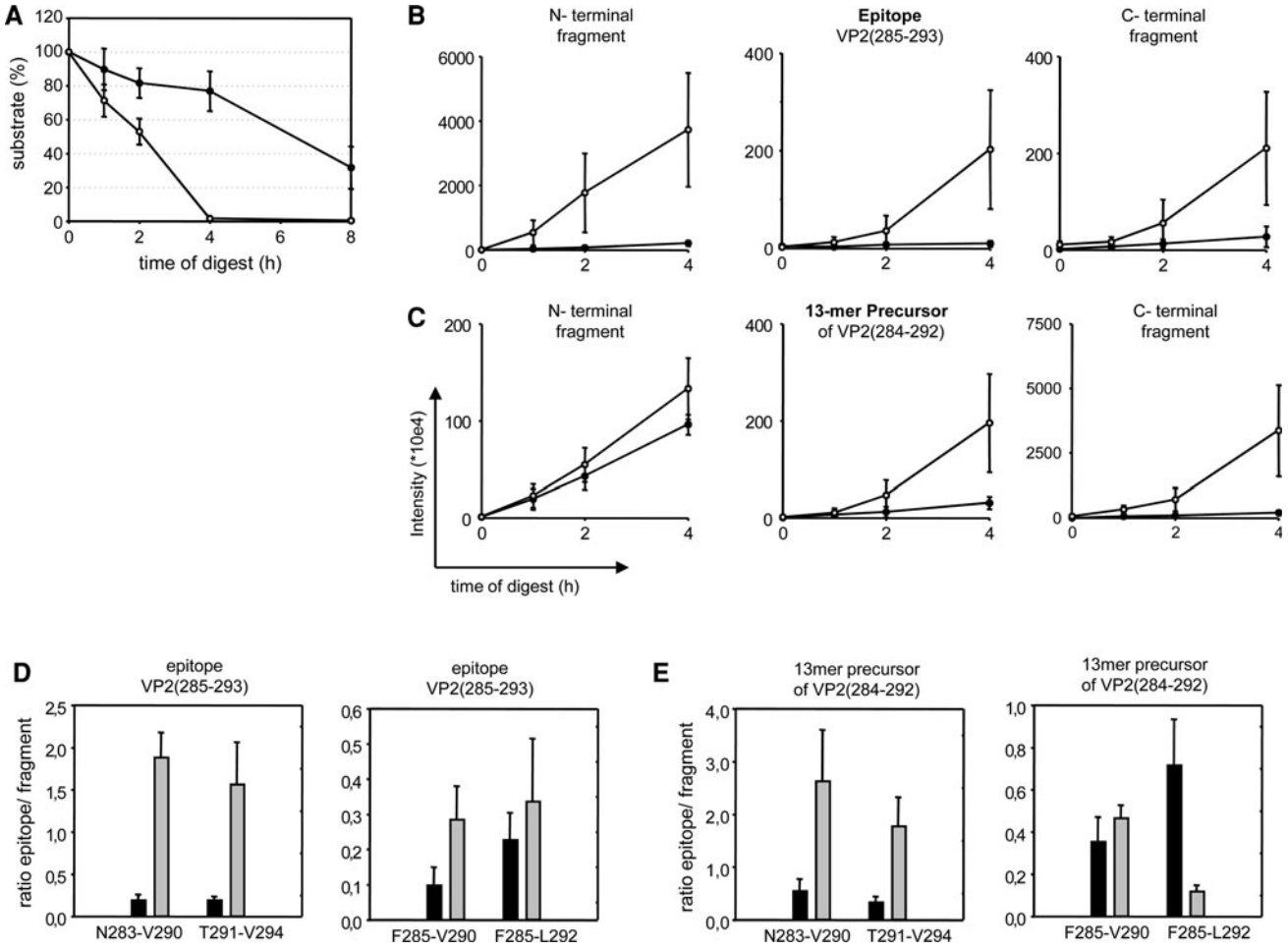

Fig. 4 Proteasomal generation of the VP2(285–293) epitope and of the VP2(284–292) precursor peptide. **a** Substrate degradation of the 31mer polypeptide $VP2_{272–302}$ by s20S and i20S is shown. **b**, **c** Results obtained from mass spectrometric analysis of proteasomal products from the $VP2_{272–302}$ substrate are shown. In vitro processing of the $VP2_{272–302}$ substrate yielded the VP2(285–293) epitope **b** and the VP2(284–292) precursor peptide **c**. Also the generation of epitope-flanking peptides is shown. s20S *filled circles* and i20S *open circles*. Also, the increase of i20S-dependent epitope/precursor generation was analyzed by standardization to simultaneously generated antitopes. All fragments intensities were estimated by ESI–MS. The ratios of normalized ion counts of the epitope VP2(285–293)/respective antitope (D) and of the VP2(284–292) precursor peptide/respective antitope (E) were calculated for each fragmentation assay [s20S *black bars* and i20S *gray bars*] at 2 h. Proteasomal cleavage behind V290 yielded the fragments N283–V290 and T291–V294. Additionally, the F285–V290 antitope [shares the N-terminus with the VP2(285–293) epitope] and the F285–L292 antitope [shares the N-terminus with the VP2(285–293) epitope and the C-terminus with the VP2(284–292) precursor] were selected for ratio calculations

Table 2 MHC affinity of VP2(273–281), VP2(284–292), and VP2(285–293)

Position in CVB3 Nancy	Sequence	SYFPEITHI score	MHC binding IC_{50} (nM) prediction	MHC affinity (in relation to LCMV FQPQNGQFI)		
				Affinity (μM)	RA (relative affinity)	DC_{50} (h)
VP2 (273)	MPYTNSVPM	22	565.5	2.41	1	2
VP2 (284)	MFRHNNVTL	21	4,569.9	22.11	10	<1
VP2 (285)	FRHNNVTLM	25	631.7	2.20	1	6

The H-$2D^b$ MHC-I affinity was determined for the VP2(273–281), VP2(284–292), and VP2(285–293) peptides. The prediction data of IC_{50} are from IEDB database (Zhang et al. 2008). The relative affinity (RA) and the MHC-I peptide complex stability (DC_{50}) were determined in RMA-S cells as described above. FQPQNGQFI from LCMV was used as a reference peptide. Affinity (μM) in the fourth column: peptide concentration of the peptide of interest at 20% of maximal binding capacity. Primarily, the VP2(285–293) peptide was identified to be a high-affine binder to MHC-I

the same manner, the overall enhanced precursor peptide generation in the i20S fragmentation study appeared not to result from different cleavage site usage by i20S. Although standardisation of the 13mer precursor peptide of VP2(284–292) to antitopes N283–V290 and T291–V294 suggested enhanced precursor peptide liberation, the ratio of the VP2(284–292) precursor peptide/F285–V290 antitope pointed to a generation of both fragments by s20S and i20S to the same extent. More important, the generation of the F285–L292 antitope was clearly preferred by i20S proteasomes (Fig. 4e), indicating overall facilitated generation of VP2(285–293) epitope and F285–L292 by i20S proteasomes.

The usage of internal peptide standards to determine the preferential generation of VP2(285–293) by i20S was also transferable to proteasomal processing studies, which were performed with proteasomes from heart, liver, small intestine and spleen with different immunoproteasome portions (Suppl. Fig. (2A)). The generation VP2(285–293) was preferred by proteasomes isolated from spleen and small intestine, thus entirely concurring with enhanced i20S content in these tissues (Suppl. Fig. (2B/C)).

MHC class I affinity of CVB3 MHC-I ligands

Table 1 depicts the predicted MHC-I scores and IC_{50} values of the potential MHC-I ligands. We tested MHC-I binding properties in MHC binding studies. FACS analysis identified the VP2(285–293) epitope to exert high MHC-I affinity. Nevertheless, the VP2(273–281) epitope, which failed to be generated by proteasomes, exerted also high affinity. In agreement with prediction scores, the VP2(284–292) peptide was shown to have low affinity to MHC-I molecules combined with a low stability to MHC-I complexes (Table 2; Suppl. Fig. (3)). Thus, the preferential generation of the VP2(285–293) epitope by i20S in addition to the high MHC-I affinity of this ligand make this epitope a likely candidate for in vivo CD8 T cell responses.

VP2(285–293)-specific T cells in CVB3-infected mice

Finally, we investigated the ability of selected peptides to stimulate T cells. We analyzed the capacity of VP2(273–281), VP2(284–292) and VP2(285–293) to stimulate the proliferation of lymphocytes from CVB3-infected mice. Peptide pools of these respective MHC-I ligands induced a weak stimulation of T cell proliferation (data not shown). Peptide stimulation was repeated with distinct peptides revealing the VP2(285–293) peptide to be the most promising candidate within this peptide pool to induce T cell proliferation (Fig. 5a). None of the other peptides induced proliferation of CD8 T cells (data not shown). To discriminate epitope-specific T cells, we performed intracellular IFN-γ staining of CD8 T cells derived from naïve (Fig. 5b) and CVB3 infected mice (Fig. 5c). Indeed, as illustrated in Fig. 5c, a small portion of VP2(285–293)-specific T cells were detected in CVB3-infected mice after exposure of T cells to antigen-presenting cells pulsed with 5 μM of the VP2(285–293) epitope. Again, we failed to detect a relevant fraction of epitope-specific T cells for VP2(273–281), VP2(284–292) and the F285–L292 antitope (data not shown). Thus, these results indicated that the VP2(285–293) peptide, which was preferentially generated by i20S and was identified to exert high affinity to MHC-I, may function as a CD8 T cell epitope in CVB3-infection.

Discussion

The remarkable role of CD8 T cells in the control of acute inflammation in CVB3-infection was particularly substantiated by the finding that MHC class I antigen presentation-deficient mice exert fulminant myocarditis and chronic disease (Klingel et al. 2003). CD8 T cell depletion studies suggested a contribution of CD8 T cells to virus elimination in CVB3-myocarditis as well (Henke et al. 1995). Knowledge of the structure of MHC-I ligands, which bind to specific CD8 T cells, may support the development of

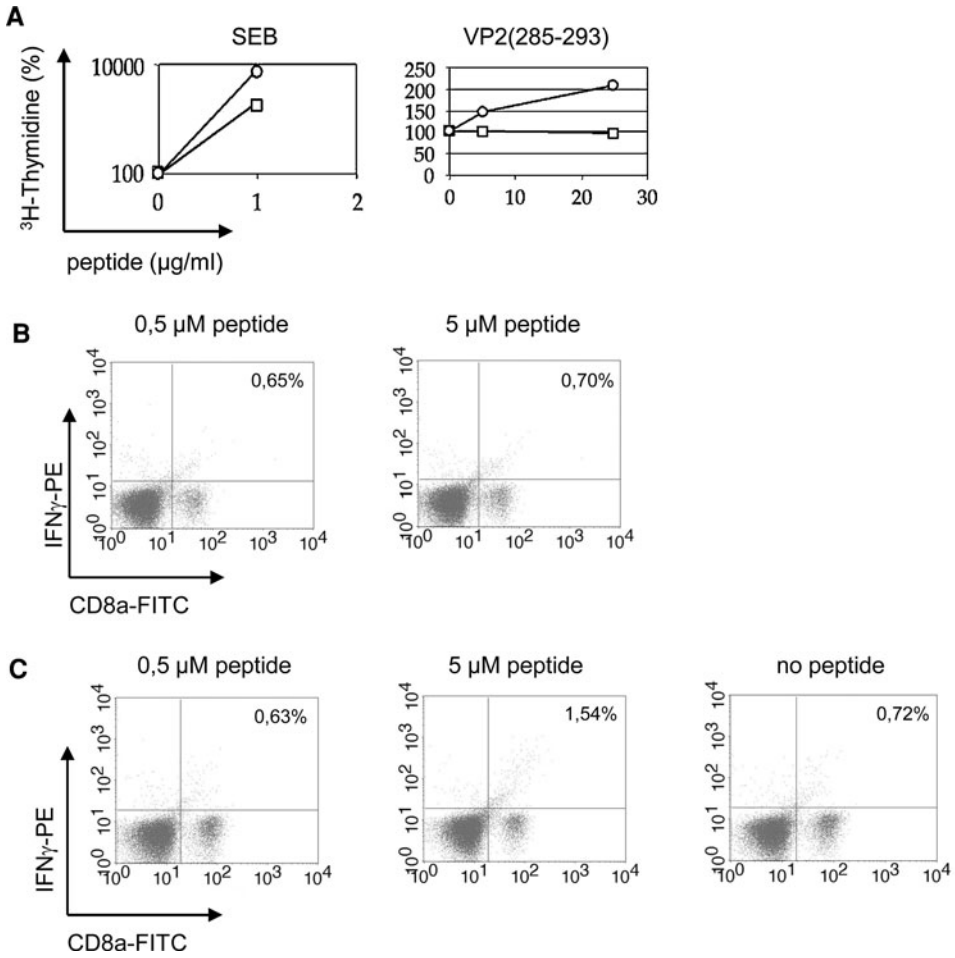

Fig. 5 VP2(285–293) is a CD8 T cell epitope. **a** T cell proliferation: Single cell suspensions derived from spleen of CVB3-infected C57BL/6 mice (day 8 p.i., *circles*) and from naïve C57BL/6 mice (*squares*) were stimulated with the VP2(285–293) peptide. The proliferation is shown as % of ^{3}H-thymidine incorporation within the last 10 h. Stimulation of proliferation by SEB was used as a control. Proliferation assays were repeated three times, one representative result with splenocytes, which were pooled from 4 mice, is shown. **b**, **c** Intracellular IFN-γ stain of epitope-specific CD8 T cells: Single cell suspensions derived from spleen of naïve C57BL/6 mice **b** and of CVB3-infected C57BL/6 mice **c** were stimulated with VP2(285–293) at two concentrations: 0.5 and 5 µM. Representative FACS stains are shown. Frequencies of IFN-γ positive CD8 T cells are indicated in the *right upper* quadrant. Results shown are representative for at least two independent experiments, which were performed with pooled splenocytes from 4 mice

specific T cell assays, and possibly the design of a stringent vaccine. In silico MHC-I prediction has been continuously challenged in the past. Companion databases combining MHC binding with proteasomal cleavage and peptide transport prediction via TAP were established, thus generating an overall processing score to determine the intrinsic potential of an individual peptide to exert T cell epitope characteristics (Larsen et al. 2005; Peters et al. 2003). Meanwhile, a few examples for successful reversed immunology approaches are known (van Endert et al. 2006). However, due to the complexity of intracellular protein processing the prediction of MHC-I ligand generation remains to be the most sophisticated part of in silico databases.

Proteasomes are known as the main supplier for MHC-I ligands, whereby predominantly the C-termini of MHC-I ligands are generated by proteasomes (Kloetzel 2001). In an approach to identify MHC-I ligands for CVB3, here we analyzed the generation of 13 in silico predicted MHC-I ligands from the CVB3-polyprotein by proteasomes in vitro. It had been shown previously that in vitro proteasomal T cell epitope generation concurs with in vivo epitope liberation (Sijts et al. 2000; Voigt et al. 2007). We focused on the generation of the correct C-terminus of MHC-I ligands and in parallel analyzed the generation of N-terminally elongated precursor peptides of CVB3. Subsequent proteolytic steps are necessary to trim N-terminally elongated peptides to meet MHC-I restrictions (Goldberg et al. 2002; York et al. 2006, 2002). In total, 13 H-2^b restricted peptides revealing a high in silico likelihood to be generated by proteasomes [11 peptides revealed a proteasome

cleavage score of ≥1.0] and to exert high or intermediate binding affinity to MHC-I molecules [SYFPEITHI ≥21] were selected for in vitro processing studies by proteasomes. This study has shown that 5 of the 13 selected CVB3 MHC-I ligands were actually generated as correct 9mer (D^b) and 8mer (K^b) epitopes by proteasomes in vitro. One limitation of the present study is the fact that predictors for proteasome cleavage are available only for the human proteasome, which may have influenced the cleavage prediction as shown here in the murine system. On the other hand, a comparison of proteasome cleavage products performed with 20S proteasome complexes derived from human and murine origin revealed only minor differences in cleavage site usage by either proteasome species for CVB3-peptides (Jakel et al. 2009).

Considering the high affinity of TAP to N-terminally elongated MHC-I ligands (Fruci et al. 2003), the generation of N-terminal precursors appears to be feasible as well. For two predicted MHC-I ligands exclusively precursor peptides were detected upon proteasome cleavage of polypeptide substrates, whereby for three of the correctly generated ligands additional precursor peptides were detected as well. These peptides may eventually be trimmed at their N-terminus by peptidases in the cytosol or within the ER (Beninga et al. 1998; Cascio et al. 2001), thus expanding the candidate pool of MHC-I ligands. However, proline residues within the first N-terminal amino acids of a generated fragment are known to interfere with efficient peptide transport by TAP (Neisig et al. 1995). Thus, in addition to low-affine binding of the VP2(284–292) epitope to MHC-I as shown here (Table 2), the transfer of the VP2(284–292) 13mer precursor peptide to the ER appears to be an unlikely event due to the proline residue at the N-terminus. Our findings of limited immunoproteasome-dependency, the low MHC-I affinity of the VP2(284–292) peptide as well as the most likely restricted peptide transport via TAP of the 13mer precursor peptide are in good agreement with the lack of VP2(284–292) epitope-specific T cells in CVB3-infection.

Although in silico prediction suggested the generation of the selected peptides by proteasomes, we failed to detect epitopes or N-terminally elongated precursors for six predicted MHC-I ligands despite the change of flanking residue lengths or improvement of substrate solubility by peptide modification. A remarkable number of predicted MHC-I ligands was found to be located within the same region revealing a partial sequence overlap of these peptides. Therefore, it seems likely that particular proteasomal cleavage eventually leads to the destruction of some epitopes, whereas the generation of others may be favored. Also, alternative proteases might generate some MHC-I epitopes alone or at least in cooperation with proteasomes (Del and Val 1997; Seifert et al. 2003), points which have not been studied here. On the other hand, our data suggest a risk of this approach to investigate false positives despite the combined approach of different prediction methods as shown here. In addition to the combined in silico prediction and in vitro proteasome digest approach to identify CVB3-epitopes, the elution of peptides from MHC class I molecules and subsequent identification by mass spectrometry was introduced recently. This more straightforward approach allows the direct identification of epitopes presented on MHC-I molecules on the cell surface (Meiring et al. 2006; Soethout et al. 2007). However, taking into account the various modes of viral immune escape exerted by CVB3 eventually resulting in MHC class I down-regulation (Cornell et al. 2006, 2007), this approach appears to be challenging in the CVB3-model. Indeed, we failed to detect any CVB3-peptide by mass spectroscopy following MHC-elution of CVB3-transfected MEK217 cells (a cell-line that expresses immunoproteasomes in tetracycline-dependency (Sijts et al. 2000); data not shown).

IFN-expression is up regulated early upon CVB3-infection in mice, which results in enhanced immunoproteasome synthesis and proteolytic function particularly in the infected myocardium (Szalay et al. 2006). Immunoproteasomes are considered to enhance the generation of antigenic peptides (Kloetzel 2001; Schwarz et al. 2000; Sijts et al. 2000; Strehl et al. 2006). Our recent study revealed a potential impact of immunoproteasome activity on the severity of myocarditis: in mice being susceptible to chronic disease, immunoproteasome-dependent CVB3 epitope generation was delayed to stages where excessive inflammation concomitant with the high viral load were already present (Jakel et al. 2009). The emerging picture of proteasomal activity reveals that early antigen-processing determines the ability of pathogen-derived peptides to elicit a CD8 T cell response (Deol et al. 2007; Strehl et al. 2006). Therefore, i20S-dependent generation of ligands or precursor peptides was of particular interest. Facilitated peptide degradation by i20S was associated with enhanced generation of the predicted VP2(285–293) epitope. To investigate, whether improved epitope generation was also due to altered cleavage sites preferences of i20S, we calculated the ratios of these generated fragments to antitopes as described previously (Strehl et al. 2008). Our data revealed a clear immunoproteasomal preference of VP2(285–293) epitope generation that was due to enhanced cleavages site usage at the N-terminus of the substrate peptide behind M284/F285 that consequently resulted in the generation of VP2(285–293) or F285–L292 8mer, but excluded the liberation of VP2(284–292) or respective precursor peptides. Both C-terminal cleavages at L292/M293 and at M293/V294 were preferentially generated by immunoproteasomes. However, in agreement with the low MHC-I binding affinity of F285–L292 to H-$2D^b$ and H-$2K^b$

molecules, no F285–L292-specific T cells were detected in CVB3-infection (data not shown). Thus, the F285–L292 antitope is competitively generated by i20S, but fails to exert an antigenic potential in CVB3 infection.

Here we have shown that VP2(285–293)-epitope specific CD8 T cells proliferate in CVB3-infection in vivo although the observed preferential generation of the VP2(285–293) epitope did not meet the computational proteasomal cleavage prediction, which suggested preferential cleavage site usage of i20S at L292/M293 (Table 1), thereby reducing VP2(285–293) epitope liberation. Thus, for optimal prediction program usage it appears essential to consider the combined scores provided by proteasomal cleavage prediction as well as those of TAP and MHC binding predictions. Indeed, the i20S-dependent generation of the VP2(285–293) epitope was in good agreement with the high MHC-I binding affinity and complex stability. In addition to data shown in Fig. 5, our recent study has disclosed VP2(285–293)-epitope specific CD8 T cells by pentamer staining and by IFN-γ secretion in antigen-presentation assays in CVB3-infection, thus substantiating an in vivo role of this H-2^b epitope (Jakel et al. 2009).

Facilitated antigen processing of CVB3 epitopes by immunoproteasomes is particularly important with respect to complex immune evasion strategies, which are exerted upon CVB3 infection. Several CVB3 proteins can limit the presentation of viral epitopes on the surface of infected cells and eventually interfere with CD4 and CD8 T-cell responses (Cornell et al. 2007; Kemball et al. 2008), thus substantiating the need for efficient antigenic peptide supply early upon CVB3-infection (Deol et al. 2007; Jakel et al. 2009). These immune escape mechanisms may also explain the relatively low overall epitope-specific CD8 T cell quantities in CVB3-infection in comparison to classic viral mouse models of CD8 T cell immunity (Jakel et al. 2009). In correspondence to the VP2(285–293) epitope, the generation of the H-$2K^b$-restricted P3D(1170–1177) epitope was also found to be immunoproteasome-dependent (data not shown), which was likewise in agreement with the detection of P3D(1170–1177)-specific T cells in CVB3-myocarditis in mice (Jakel et al. 2009). In addition to our data in mice a recent study disclosed an immunodominant CD8 T cell epitope also in human beings: the HLA-A*02-restricted epitope ILMNDQEVGV was recognized by 25% of all tested blood donors. The prevalence of these epitope-specific T cells may contribute to the protection from a potential chronic course of myocarditis (Weinzierl et al. 2008), thus emphasizing the protective role of CD8 T cells in CVB3 infection.

In conclusion, in silico prediction of murine CVB3 MHC-I ligands is a useful tool for the initial selection of $CD8^+$ T cell epitope candidates. In addition to high MHC-I binding affinities of generated epitopes, a sufficient peptide amount early upon infection, which is provided by immunoproteasome activity upon cytokine induction, appears to be involved in the effective interaction of MHC-I presenting cells with T cells. As shown here, the cellular protein supply remains to be the most challenging part of in silico CVB3 MHC-I ligand prediction, thus emphasizing the demand for in vitro proteasomal processing studies to analyze CVB3 epitope generation. The combination of in silico prediction methods, in vitro digests with s20S and i20S proteasomes, in vitro MHC binding studies and in vivo testing eventually resulted in the identification of CVB3 MHC-I epitopes.

Materials and methods

Prediction methods

The CVB3 protein sequence was obtained from the SwissProt database http://expasy.ch. The UniProtKB/SwissProt accession number of CVB3 Polyprotein is P03313.

SYFPEITHI is a database of MHC ligands and peptide motifs, which is implemented online at http://www.syfpeithi.de (Rammensee et al. 1999). This database assigns an overall likelihood of a peptide of being a natural MHC ligand (Rammensee et al. 1999), the threshold for the inclusion of peptides into our study is described in the result section..

Immune epitope database analysis resource provides access to well-documented and tested epitope-related tools through a common style of web interface: http://tools.immuneepitope.org/main/html/tcell_tools.html (Zhang et al. 2008). For search of MHC class I ligand by IEDB-AR we used the stabilized matrix method (smm). Smm combines the prediction values of the individual steps of antigen presentation, i.e. proteasomal peptide processing, transport into the ER via TAP and the fulfilling of MHC class I binding criteria, to give an overall score for each peptide's intrinsic potential of being a T cell epitope (Peters and Sette 2005; Tenzer et al. 2005). The MHC binding predicted value is given as $-\log(IC50)$. All scores associate higher values with higher predicted efficiency. MHC affinity is shown as IC_{50} (nM): IC_{50} <50 for high affine binder, IC_{50} <500 for intermediate affine binder and IC_{50} >5,000 for low affine binder. For proteasome cleavage prediction two implementations are provided in IEDB-AR, one based on matrices (which was used here) and one on neural networks (NetChop and NetCTL). The scores in Table 1 can be interpreted as logarithms of the total amount of cleavage site usage liberating the peptide C-terminus.

Proteasome purification

Proteasomes were isolated according to standard procedures (Voigt et al. 2007). Standard proteasomes were isolated from T2 cells and immunoproteasomes from T27mp cells as described previously (Kuckelkorn et al. 2002; Voigt et al. 2007). Organs from naïve C57BL/6 mice were homogenized in 20 mM Tris, pH 7.2, 1 mM EDTA, 1 mM NaN_3, 1 mM DTT, 0.5% NP40, protease-inhibitor cocktail (Complete®, Roche). Further purification was performed according to (Kuckelkorn et al. 2002; Szalay et al. 2006). Incorporation of immunosubunits was controlled by immunoblot analysis as described previously (Kuckelkorn et al. 2002). Antibodies used for immunoblot were: ab3328 (Abcam) and #62966 (β1i), K63/5 (β5i), K65/4 (β2i).

Peptide synthesis

Peptides harboring the predicted epitopes were synthesized using standard Fmoc methodology (0.1 mmol) on an Applied Biosystems 433A automated synthesizer. The peptides were purified by HPLC and analyzed by mass spectrometry (ABI Voyager DE PRO).

In vitro degradation and mass spectrometry analysis of peptides

Polypeptides (10 µg) harboring predicted MHC class I ligands were incubated with 20S proteasomes (1–2 µg) in 20 mM Hepes, pH 7.8, 2 mM Mg-acetate, 2 mM DTT at 37°C for the indicated time points. Reactions were stopped by 0.3% TFA. Samples were analyzed by RP-HPLC; the HP1100 system (Hewlett-Packard, Germany) equipped with a RPC C2/C18 SC 2.1/10 column (GE Healthcare, Germany). Analysis was performed online with a LCQ ion trap MS equipped with an electro spray ion source (Thermo Fisher Scientific, Germany). Ion counts of each reaction were normalized to the 9GPS standard peptide, which was added in equal amounts prior to analysis. To determine whether fragment generation is the result of enhanced turnover rate or of altered cleavage preference of i20S, epitope peptides were related to so-called antitope peptides (Kuckelkorn et al. 2002). Data are shown as mean of at least three independent experiments ±SEM.

Flow cytometric analysis of H-2K^b and H-2D^b molecules

Relative affinity (RA) of peptides to MHC class I and stability (DC_{50}) of MHC class I ligands complexes were determined as described elsewhere (Tourdot et al. 2000). For affinity studies, stripped RMA-S cells were incubated with various peptide concentrations (100, 50, 5, 2.5, 0.5 µg/ml) 2 h in serum-free medium supplemented with 1.5 µg/ml β_2 microglobulin. For MHC class I stability RMA-S cells were incubated with 100 µg/ml peptide overnight, washed and cultured in the presence of Brefeldin A for 0, 2, 4, 6 and 8 h. All cells were stained with H-2D^b-PE (BD clone: KH95) and H-2K^b-PE (BD clone: AF6-88.5) mAb.

Relative affinity

Maximal binding capacity is defined as binding of a reference peptide at 100 µM. RA was determined for each peptide concentration as follows: RA = peptide concentration of peptide of interest at 20% of maximal binding capacity/peptide concentration of reference peptide at 20% of maximal binding capacity. A low RA (RA < 10) suggest high affine binding of peptides to MHC class I molecules.

MHC complex stability

Dissociation complex DC_{50} is defined as the time needed to destabilize 50% of initially formed peptide/MHC complexes at time $t = 0$ h. A higher DC_{50} suggests a more stable complex.

Infection of mice with CVB3

CVB3 (cardiotropic Nancy strain) used in this study was prepared as previously described (Kandolf and Hofschneider 1985). C57BL/6 mice (H-2^b haplotype) were kept at the animal facilities of the Charité University Medical Center and at the Institute of Pathology at the University of Tübingen. All experiments were conducted according to the German Animal Protection Act. Six weeks old were infected i.p. with 1×10^5 PFU of purified CVB3 as described previously (Szalay et al. 2006).

Proliferation assay

2×10^5 cells derived from spleen of infected (day 8 p.i.) and non-infected C57BL/6 mice [pool of 4 mice] were incubated with 5 or 25 µg/ml peptide for 72 h at 37°C. 1 µg/ml Enterotoxin B from *Staphylococcus aureus* (SEB) stimulation served as a positive control. 18 h before the incubation was finished 1 µCi ^{3}H-thymidine was added. Subsequently, cells were transferred onto scintillation plates with Packard Harvester Filtermate 196 (Packard) according to manufactures' protocols. Incorporated ^{3}H was counted with the Liquid Scintillation counter Wallac 1410 (Wallac).

Intracellular cytokine stain

1×10^6 spleen cells derived from CVB3 infected C57Bl6 mice were incubated with 0.5 or 5 μM peptide for 10 h at 37°C. 4 h before incubation was stopped 5 μg/ml Brefeldin A (BFA) was added. Cells were washed with PBS/1%BSA and blocked with 15 μg/ml anti-Fcγ- receptor for 10 min in ice followed by incubation with anti-CD8a-FITC for 30 min. Cells were washed twice with PBS/1% BSA and were fixed with 2% paraformaldehyde. Subsequently cells were washed with 0.1% saponin/PBS and incubated with anti-IFNγ-PE in 0.1% saponin for 30 min in ice; cells were washed and analyzed with FACS Calibur (BD) and evaluated with CellQuestPro.

Statistics

Results of continuous variables are expressed as mean ± standard error of mean (SEM). Two group comparisons of non-parametric data were performed using the Mann–Whitney test. The *t* test was used for normally distributed variables. Significance was assessed at the $p < 0.05$ level.

Acknowledgments This study was supported by the Deutsche Forschungsgemeinschaft: SFB/TR 19 to A.V., U.K., P.K., K.K. and SFB 421 to P.K. The authors have no conflicting financial interests.

References

Aki M, Shimbara N, Takashina M, Akiyama K, Kagawa S, Tamura T, Tanahashi N, Yoshimura T, Tanaka K, Ichihara A (1994) Interferon-gamma induces different subunit organizations and functional diversity of proteasomes. J Biochem 115:257–269

Beninga J, Rock KL, Goldberg AL (1998) Interferon-gamma can stimulate post-proteasomal trimming of the N terminus of an antigenic peptide by inducing leucine aminopeptidase. J Biol Chem 273:18734–18742

Cascio P, Hilton C, Kisselev AF, Rock KL, Goldberg AL (2001) 26S proteasomes and immunoproteasomes produce mainly N-extended versions of an antigenic peptide. EMBO J 20:2357–2366

Chen WS, Norbury CC, Cho YJ, Yewdell JW, Bennink JR (2001) Immunoproteasomes shape immunodominance hierarchies of antiviral CD8(+) T cells at the levels of T cell repertoire and presentation of viral antigens. J Exp Med 193:1319–1326

Cornell CT, Kiosses WB, Harkins S, Whitton JL (2006) Inhibition of protein trafficking by coxsackievirus B3: multiple viral proteins target a single organelle. J Virol 80:6637–6647

Cornell CT, Mosses WB, Harkins S, Whitton L (2007) Coxsackievirus B3 proteins directionally complement each other to downregulate surface major histocompatibility complex class I. J Virol 81:6785–6797

Deol P, Zaiss DMW, Monaco JJ, Sijts AJAM (2007) Rates of processing determine the immunogenicity of immunoproteasome-generated epitopes. J Immunol 178:7557–7562

Fruci D, Lauvau G, Saveanu L, Amicosante M, Butler RH, Polack A, Ginhoux F, Lemonnier F, Firat H, van Endert PM (2003) Quantifying recruitment of cytosolic peptides for HLA class I presentation: impact of TAP transport. J Immunol 170:2977–2984

Goldberg AL, Cascio P, Saric T, Rock KL (2002) The importance of the proteasome and subsequent proteolytic steps in the generation of antigenic peptides. Mol Immunol 39:147–164

Griffin TA, Nandi D, Cruz M, Fehling HJ, Van Kaer L, Monaco JJ, Colbert RA (1998) Immunoproteasome assembly: cooperative incorporation of interferon gamma (IFN-gamma)-inducible subunits. J Exp Med 187:97–104

Groll M, Ditzel L, Lowe J, Stock D, Bochtler M, Bartunik HD, Huber R (1997) Structure of 20S proteasome from yeast at 2.4 angstrom resolution. Nature 386:463–471

Henke A, Huber S, Stelzner A, Whitton JL (1995) The role of Cd8(+) T-lymphocytes in Coxsackievirus B3-induced myocarditis. J Virol 69:6720–6728

Jakel S, Kuckelkorn U, Szalay G, Plotz M, Textoris-Taube K, Opitz E, Klingel K, Stevanovic S, Kandolf R, Kotsch K, Stangl K, Kloetzel PM, Voigt A (2009) Differential interferon responses enhance viral epitope generation by myocardial immunoproteasomes in murine enterovirus myocarditis. Am J Pathol 175: 510–518

Kandolf R, Hofschneider PH (1985) Molecular-cloning of the genome of a cardiotropic coxsackie-B3 virus—full-length reverse-transcribed recombinant cdna generates infectious virus in mammalian-cells. Proc Natl Acad Sci USA 82:4818–4822

Kemball CC, Harkins S, Whitton JL (2008) Enumeration and functional evaluation of virus-specific CD4(+) and CD8(+) T cells in lymphoid and peripheral sites of coxsackievirus B3 infection. J Virol 82:4331–4342

Kisselev AF, Akopian TN, Woo KM, Goldberg AL (1999) The sizes of peptides generated from protein by mammalian 26 and 20 S proteasomes—implications for understanding the degradative mechanism and antigen presentation. J Biol Chem 274: 3363–3371

Klingel K, Hohenadl C, Canu A, Albrecht M, Seemann M, Mall G, Kandolf R (1992) Ongoing enterovirus-induced myocarditis is associated with persistent heart-muscle infection—quantitative-analysis of virus-replication, tissue-damage, and inflammation. Proc Natl Acad Sci USA 89:314–318

Klingel K, Schnorr JJ, Sauter M, Szalay G, Kandolf R (2003) Beta 2-microglobulin-associated regulation of interferon-gamma and virus-specific immunoglobulin G confer resistance against the development of chronic coxsackievirus myocarditis. Am J Pathol 162:1709–1720

Kloetzel PM (2001) Antigen processing by the proteasome. Nat Rev Mol Cell Biol 2:179–187

Kuckelkorn U, Ferreira EA, Drung I, Liewer U, Kloetzel PM, Theobald M (2002a) The effect of the interferon-gamma-inducible processing machinery on the generation of a naturally tumor-associated human cytotoxic T lymphocyte epitope within a wild-type and mutant p53 sequence context. Eur J Immunol 32:1368–1375

Kuckelkorn U, Ruppert T, Strehl B, Jungblut PR, Zimny-Arndt U, Lamer S, Prinz I, Drung I, Kloetzel PM, Kaufmann SHE, Steinhoff U (2002b) Link between organ-specific antigen processing by 20S proteasomes and CD8(+) T cell-mediated autoimmunity. J Exp Med 195:983–990

Kuttler C, Nussbaum AK, Dick TP, Rammensee HG, Schild H, Hadeler KP (2000) An algorithm for the prediction of proteasomal cleavages. J Mol Biol 298:417–429

Larsen MV, Lundegaard C, Lamberth K, Buus S, Brunak S, Lund O, Nielsen M (2005) An integrative approach to CTL epitope prediction: a combined algorithm integrating MHC class I binding, TAP transport efficiency, and proteasomal cleavage predictions. Eur J Immunol 35:2295–2303

Liu PP, Mason JW (2001) Advances in the understanding of myocarditis. Circulation 104:1076–1082

Lopez D, Del Val M (1997) Cutting edge: selective involvement of proteasomes and cysteine proteases in MHC class I antigen presentation. J Immunol 159:5769–5772

Mason JW (2003) Myocarditis and dilated cardiomyopathy: an inflammatory link. Cardiovasc Res 60:5–10

Meiring HD, Soethout EC, Poelen MCM, Mooibroek D, Hoogerbrugge R, Timmermans H, Boog CJ, Heck AJR, De Jong APJM, Van Els CACM (2006) Stable isotope tagging of epitopes—a highly selective strategy for the identification of major histocompatibility complex class I-associated peptides induced upon viral infection. Mol Cell Proteom 5:902–913

Neisig A, Roelse J, Sijts AJAM, Ossendorp F, Feltkamp MCW, Kast WM, Melief CJM, Neefjes JJ (1995) Major differences in transporter associated with antigen presentation (Tap)-dependent translocation of MHC class i-presentable peptides and the effect of flanking sequences. J Immunol 154:1273–1279

Peters B, Sette A (2005) Generating quantitative models describing the sequence specificity of biological processes with the stabilized matrix method. BMC Bioinf 6:132

Peters B, Bulik S, Tampe R, van Endert PM, Holzhutter HG (2003) Identifying MHC class I epitopes by predicting the TAP transport efficiency of epitope precursors. J Immunol 171: 1741–1749

Princiotta MF, Finzi D, Qian SB, Gibbs J, Schuchmann S, Buttgereit F, Bennink JR, Yewdell JW (2003) Quantitating protein synthesis, degradation, and endogenous antigen processing. Immunity 18:343–354

Rammensee HG, Bachmann J, Emmerich NPN, Bachor OA, Stevanovic S (1999) SYFPEITHI: database for MHC ligands and peptide motifs. Immunogenetics 50:213–219

Rechsteiner M, Hoffman L, Dubiel W (1993) The multicatalytic and 26-S proteases. J Biol Chem 268:6065–6068

Schwarz K, van den Broek M, Kostka S, Kraft R, Soza A, Schmidtke G, Kloetzel PM, Groettrup M (2000) Overexpression of the proteasome subunits LMP2, LMP7, and MECL-1, but not PA28 alpha/beta, enhances the presentation of an immunodominant lymphocytic choriomeningitis virus T cell epitope. J Immunol 165:768–778

Seifert U, Maranon C, Shmueli A, Desoutter JF, Wesoloski L, Janek K, Henklein P, Diescher S, Andrieu M, de la Salle H, Weinschenk T, Schild H, Laderach D, Galy A, Haas G, Kloetzel PM, Reiss Y, Hosmalin A (2003) An essential role for tripeptidyl peptidase in the generation of an MHC class I epitope. Nat Immunol 4:375–379

Sijts AJAM, Ruppert T, Rehermann B, Schmidt M, Koszinowski U, Kloetzel PM (2000a) Efficient generation of a hepatitis B virus cytotoxic T lymphocyte epitope requires the structural features of immunoproteasomes. J Exp Med 191:503–513

Sijts AJAM, Standera S, Toes REM, Ruppert T, Beekman NJCM, van Veelen PA, Ossendorp FA, Melief CJM, Kloetzel PM (2000b) MHC class I antigen processing of an Adenovirus CTL epitope is linked to the levels of immunoproteasomes in infected cells. J Immunol 164:4500–4506

Soethout EC, Meiring HD, De Jong APJM, Van Els UACM (2007) Identifying the epitope-specific T cell response to virus infections. Vaccine 25:3200–3203

Strehl B, Joeris T, Rieger M, Visekruna A, Textoris-Taube K, Kaufmann SHE, Kloetzel PM, Kuckelkorn U, Steinhoff U (2006) Immunoproteasomes are essential for clearance of *Listeria monocytogenes* in nonlymphoid tissues but not for induction of bacteria-specific CD8(+) T cells. J Immunol 177:6238–6244

Strehl B, Textoris-Taube K, Jakel S, Voigt A, Henklein P, Steinhoff U, Kloetzel PM, Kuckelkorn U (2008) Antitopes define preferential proteasomal cleavage site usage. J Biol Chem 283:17891–17897

Su RC, Miller RG (2001) Stability of surface H-2K(b), H-2D(b), and peptide-receptive H-2K(b) on splenocytes. J Immunol 167: 4869–4877

Szalay G, Meiners S, Voigt A, Lauber J, Spieth C, Speer N, Sauter M, Kuckelkorn U, Zell A, Klingel K, Stangl K, Kandolf R (2006) Ongoing coxsackievirus myocarditis is associated with increased formation and activity of myocardial immunoproteasomes. Am J Pathol 168:1542–1552

Tenzer S, Peters B, Bulik S, Schoor O, Lemmel C, Schatz MM, Kloetzel PM, Rammensee HG, Schild H, Holzhutter HG (2005) Modeling the MHC class I pathway by combining predictions of proteasomal cleavage, TAP transport and MHC class I binding. Cell Mol Life Sci 62:1025–1037

Toes REM, Nussbaum AK, Degermann S, Schirle M, Emmerich NPN, Kraft M, Laplace C, Zwinderman A, Dick TP, Muller J, Schonfisch B, Schmid C, Fehling HJ, Stevanovic S, Rammensee HG, Schild H (2001) Discrete cleavage motifs of constitutive and immunoproteasomes revealed by quantitative analysis of cleavage products. J Exp Med 194:1–12

Tourdot S, Scardino A, Saloustrou E, Gross DA, Pascolo S, Cordopatis P, Lemonnier FA, Kosmatopoulos K (2000) A general strategy to enhance immunogenicity of low-affinity HLA-A2.1-associated peptides: implication in the identification of cryptic tumor epitopes. Eur J Immunol 30:3411–3421

van Endert P, Hassainya Y, Lindo V, Bach JM, Blancou P, Lemonnier F, Mallone R (2006) HLA class I epitope discovery in type 1 diabetes. Ann N Y Acad Sci 1079:190–197

Voges D, Zwickl P, Baumeister W (1999) The 26S proteasome: a molecular machine designed for controlled proteolysis. Ann Rev Biochem 68:1015–1068

Voigt A, Salzmann U, Seifert U, Dathe M, Soza A, Kloetzel PM, Kuckelkorn U (2007) 20S proteasome-dependent generation of an IEpp89 murine cytomegalovirus-derived H-2L(d) epitope from a recombinant protein. Biochem Biophys Res Com 355:549–554

Weinzierl AO, Rudolf D, Maurer D, Wernet D, Rarnmensee HG, Stevanovic S, Klingel K (2008) Identification of HLA-A*01-and HLA-A*02-restricted CD8(+) T-cell epitopes shared among group B enteroviruses. J Gen Virol 89:2090–2097

York IA, Chang SC, Saric T, Keys JA, Favreau JM, Goldberg AL, Rock KL (2002) The ER aminopeptidase ERAP1 enhances or limits antigen presentation by trimming epitopes to 8–9 residues. Nat Immunol 3:1177–1184

York IA, Brehm MA, Zendzian S, Towne CF, Rock KL (2006) Endoplasmic reticulum aminopeptidase 1 (ERAP1) trims MHC class I-presented peptides in vivo and plays an important role in immunodominance. Proc Natl Acad Sci USA 103:9202–9207

Zhang Q, Wang P, Kim Y, Haste-Andersen P, Beaver J, Bourne PE, Bui HH, Buus S, Frankild S, Greenbaum J, Lund O, Lundegaard C, Nielsen M, Ponomarenko J, Sette A, Zhu Z, Peters B (2008) Immune epitope database analysis resource (IEDB-AR). Nucleic Acid Res 36:W513–W518